Improving our understanding of the Sun:

the role of simulations and their validation to model our star

Dr. Allan Sacha Brun
Department of Astrophysics
CEA-Paris Saclay

with: Dr. A. Strugarek, Dr. B. Perri, Dr. M. Delorme and ERC Whole Sun team

cea irfu ercWHOLE

THE ACTIVE SUN

(UV WAVELENGTH)

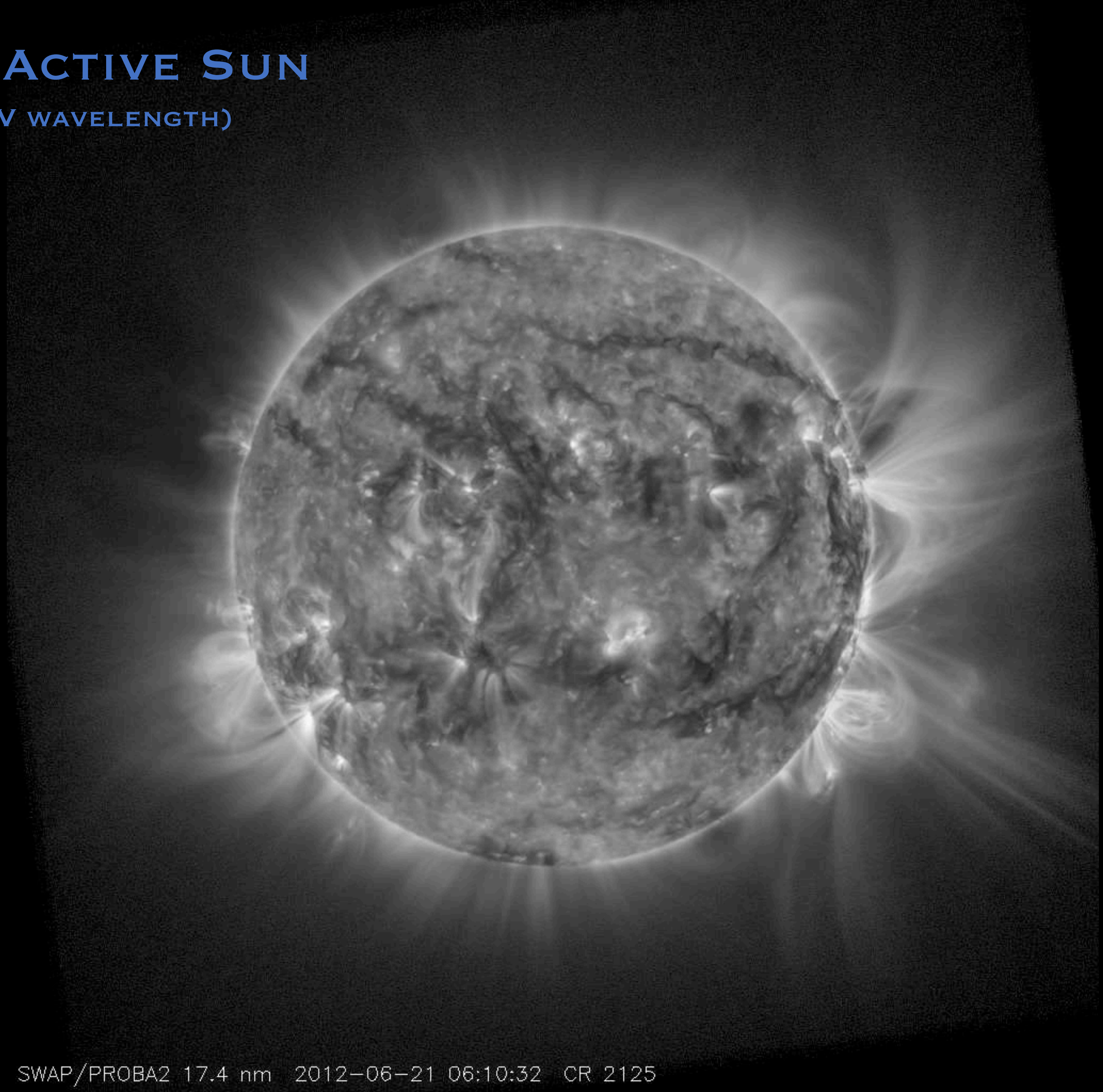

The Active Sun

(while light)

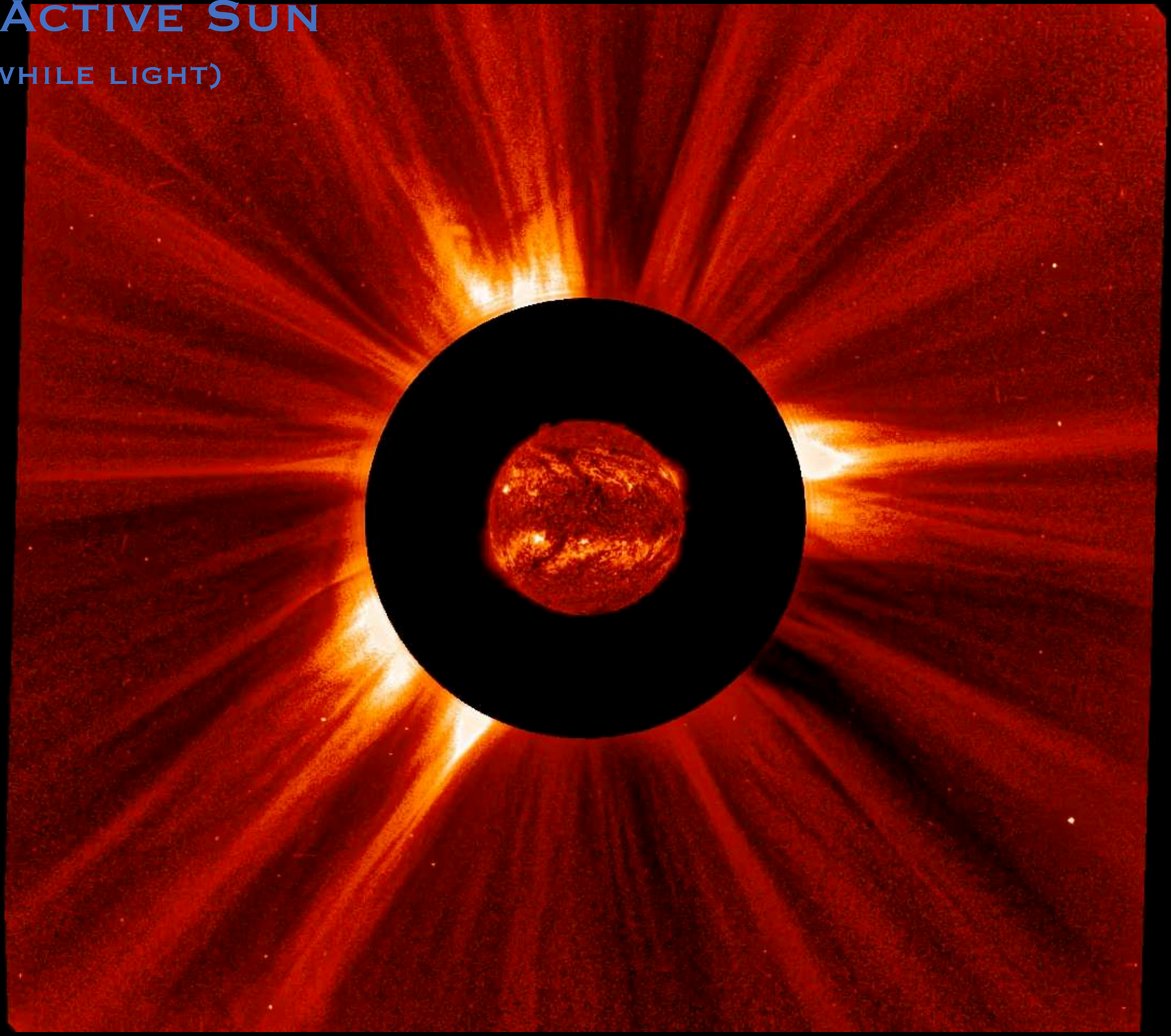

The Active Sun

(multi instruments)

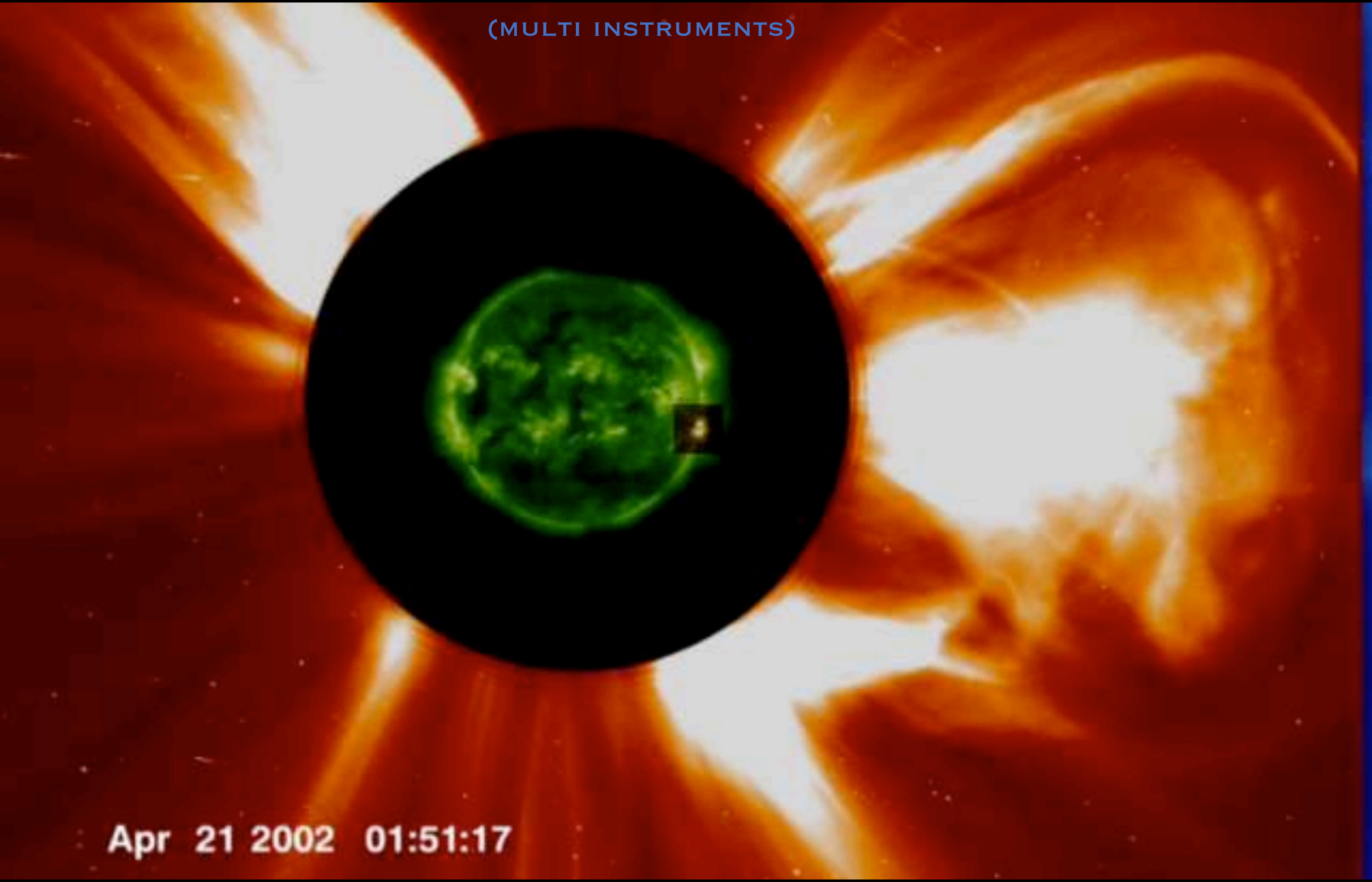

Active Sun in the Solar System

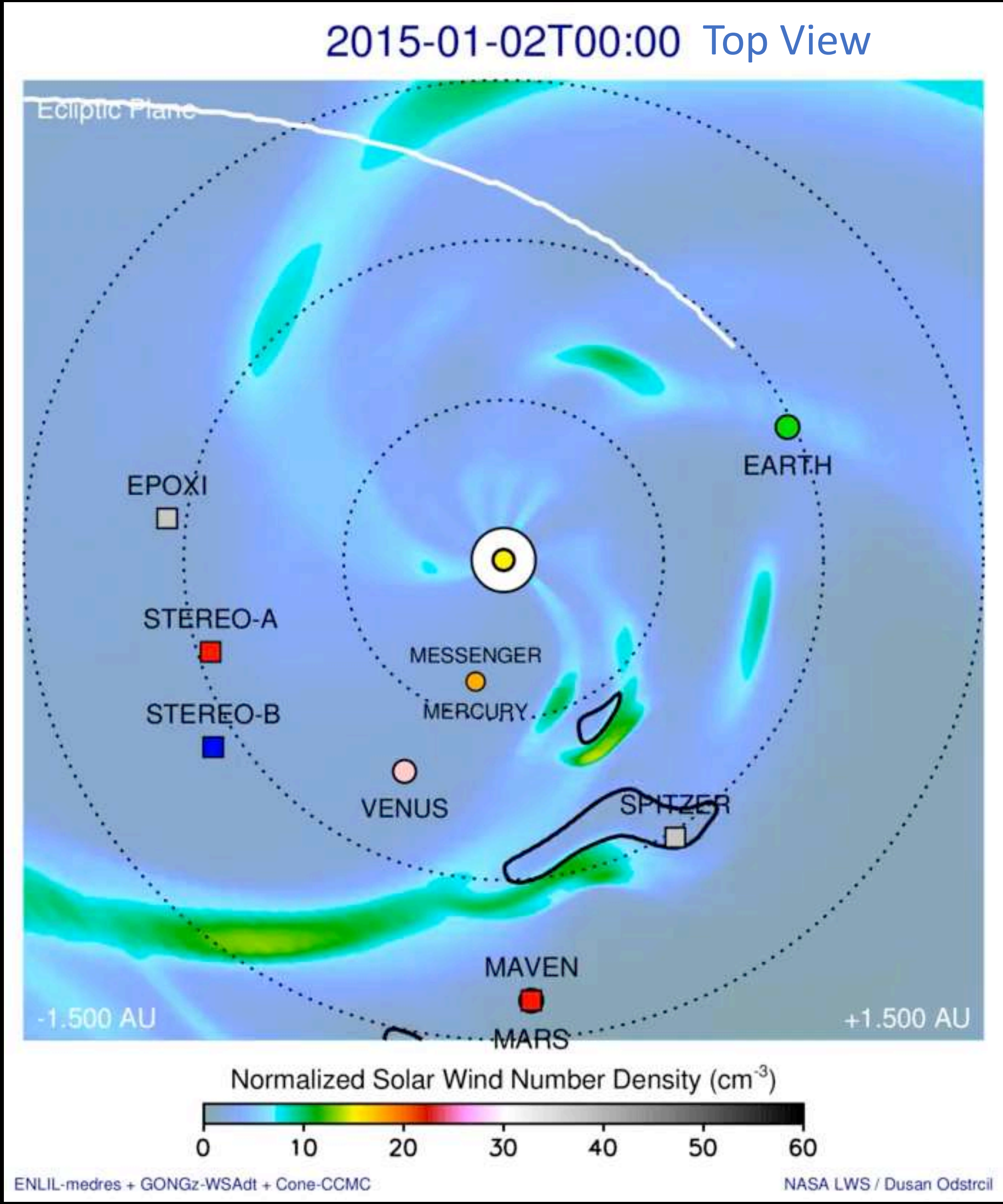

WSA-ENLIL/NOAA

SOLAR MAGNETIC CYCLE ~11 YR

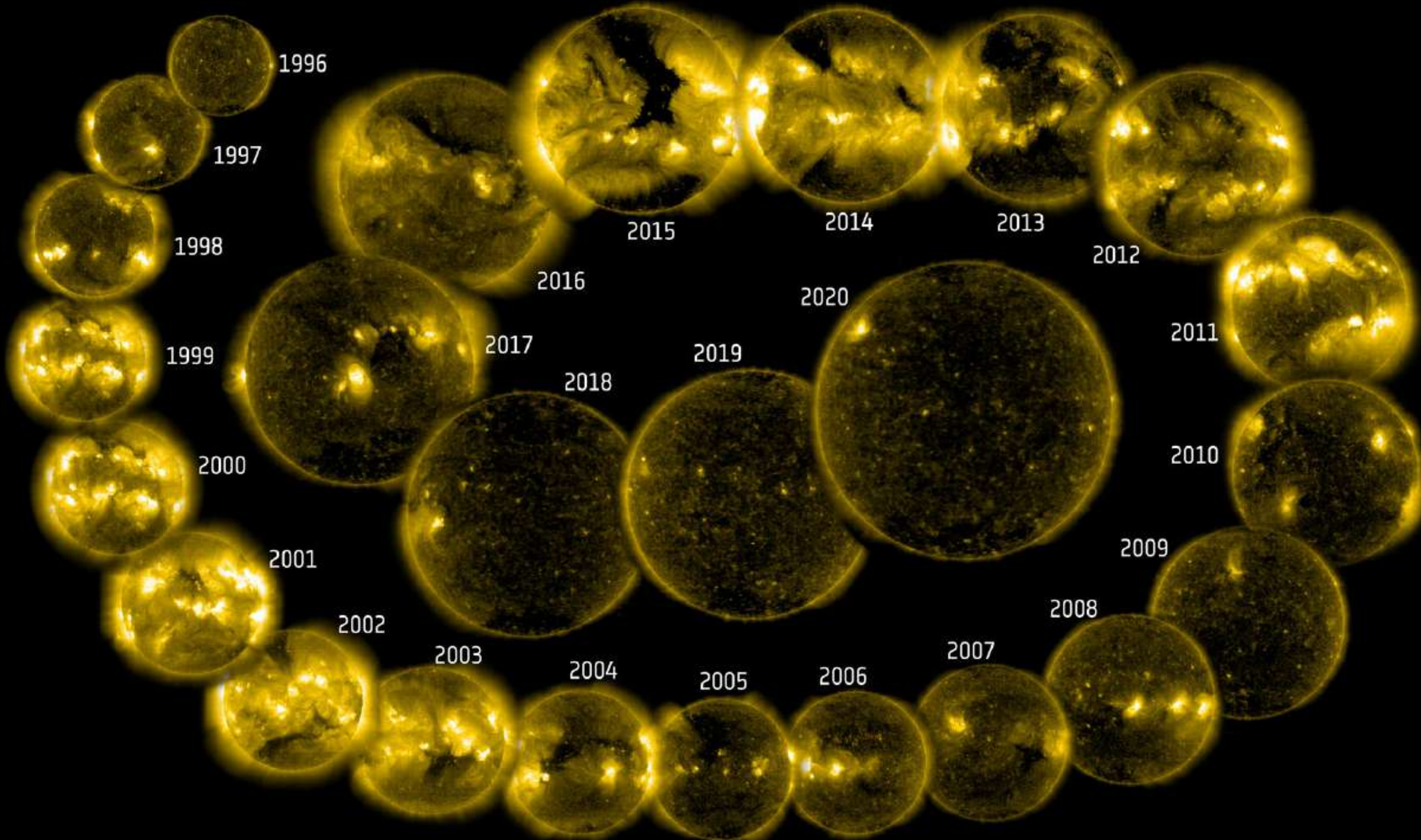

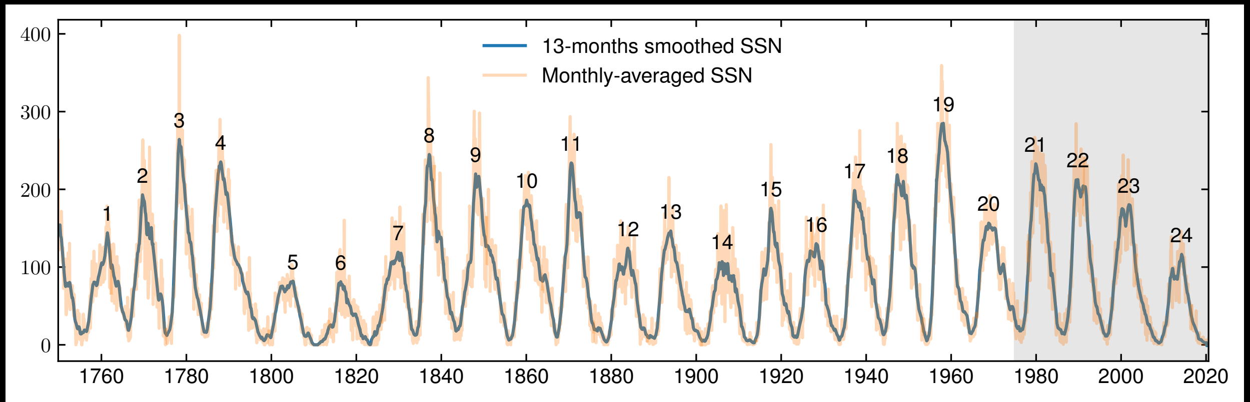

Solar Convection and Dynamo

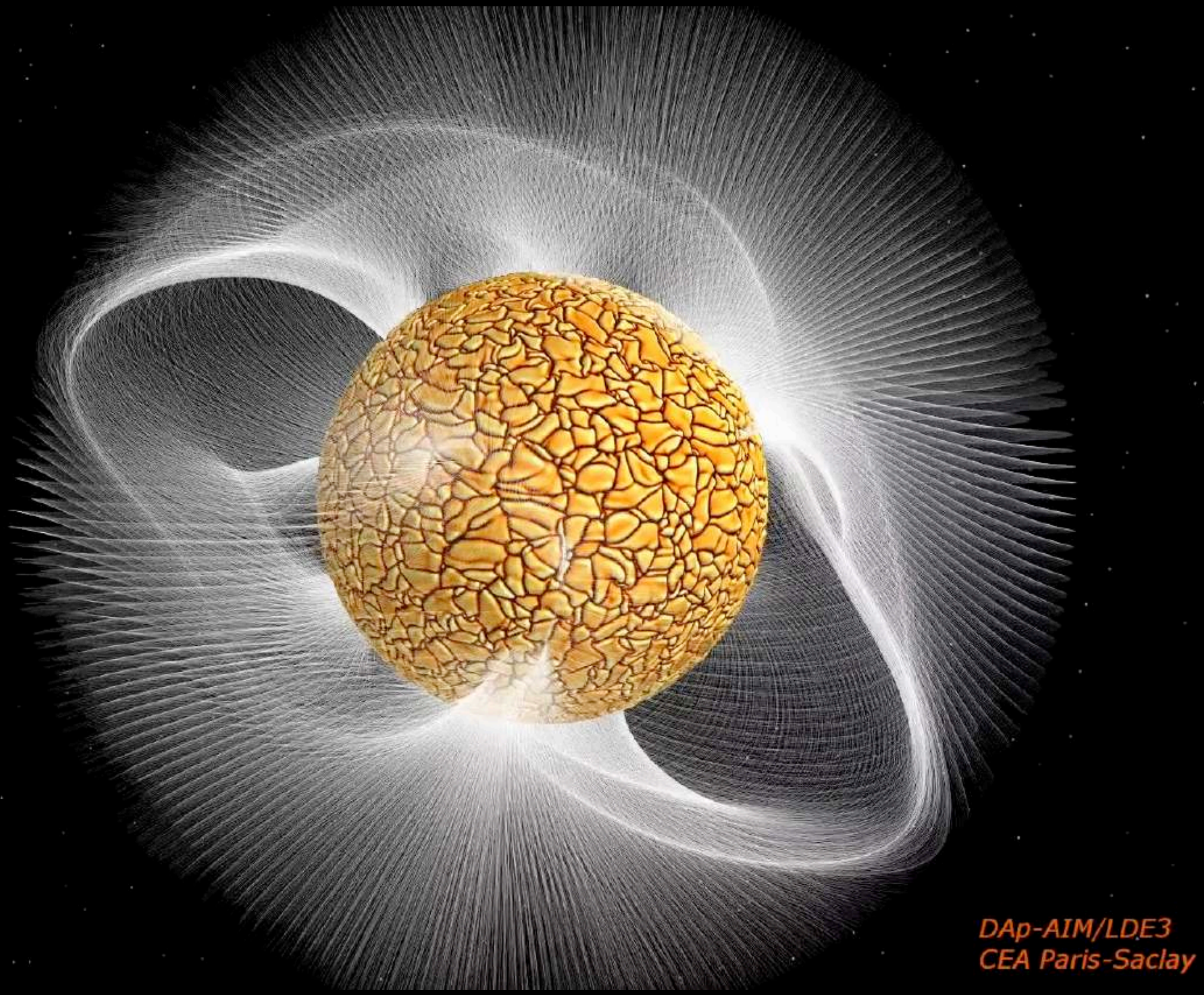

Noraz, Brun , Strugarek 2023

2nd Solar Orbiter Perihelion (February 2021)

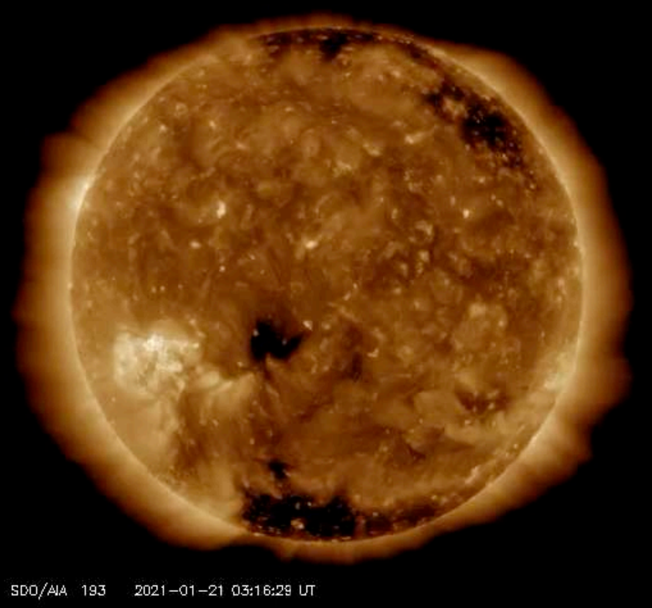

Collab: AIM/IAS/IRAP

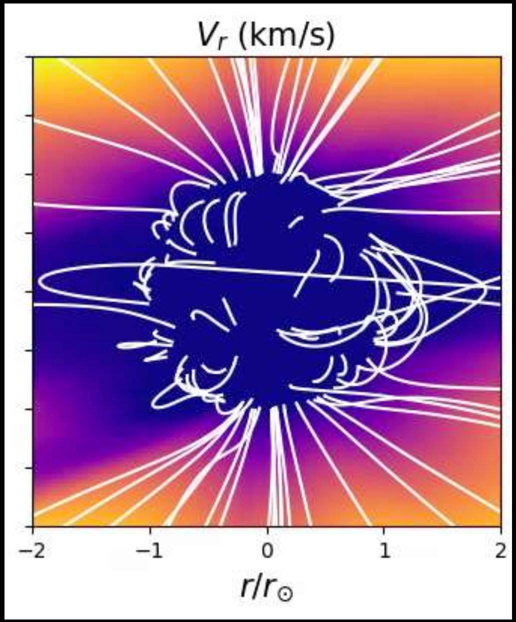

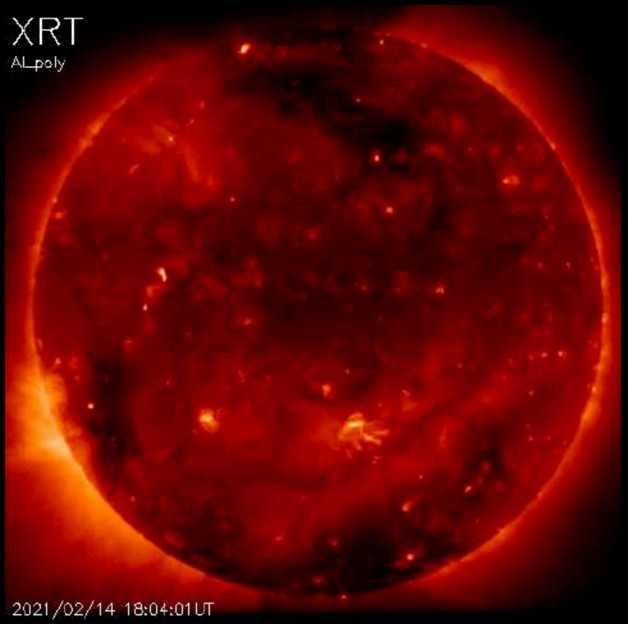

Perri et al. 2021, 2023
Parenti et al. 2022
Réville et al. 2022

Extending to Stellar Wind & Star-ExoPlanet Interactions

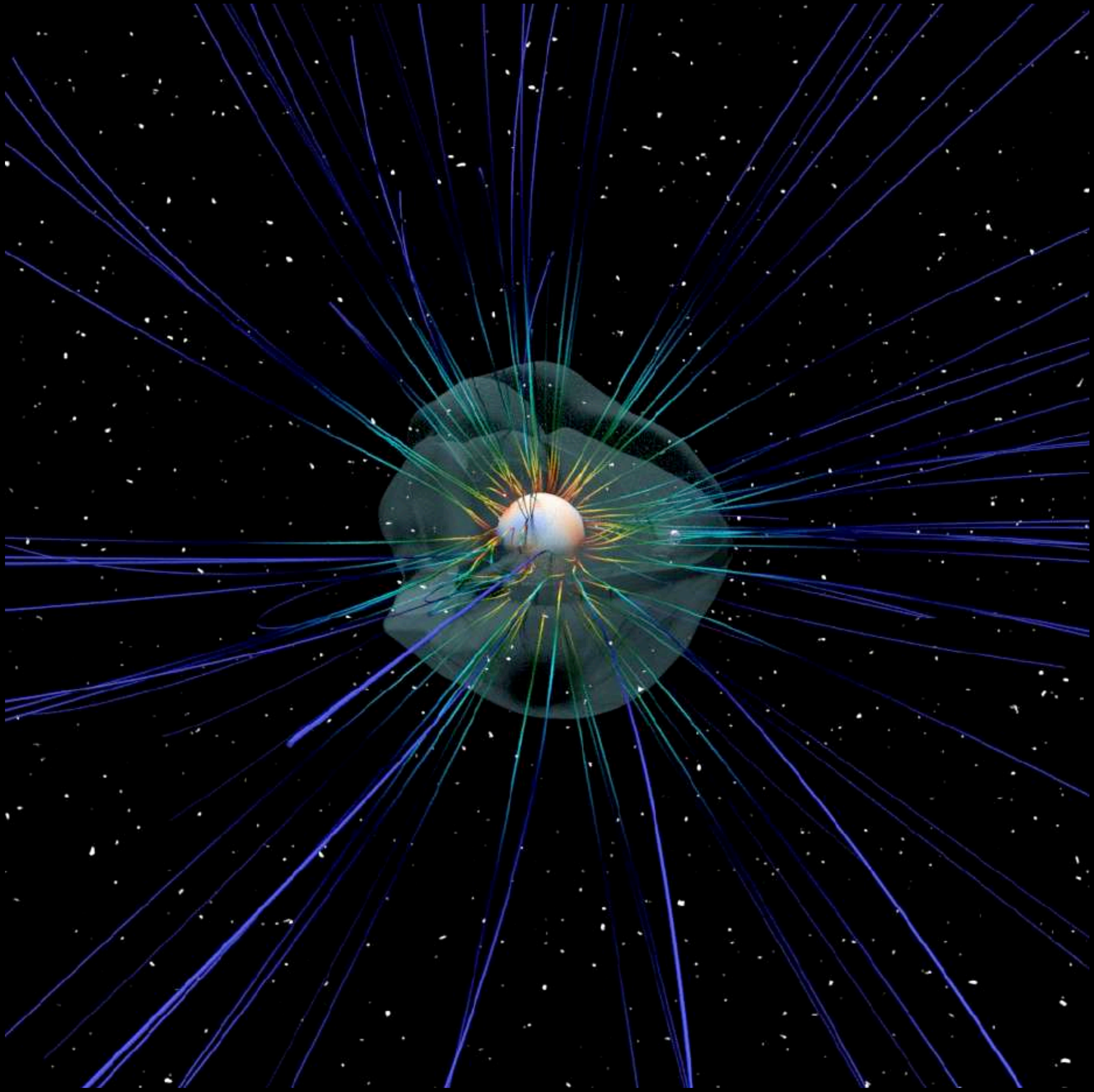

Strugarek, Brun et al. 2022

A technological society sensitive to Earth's space environment

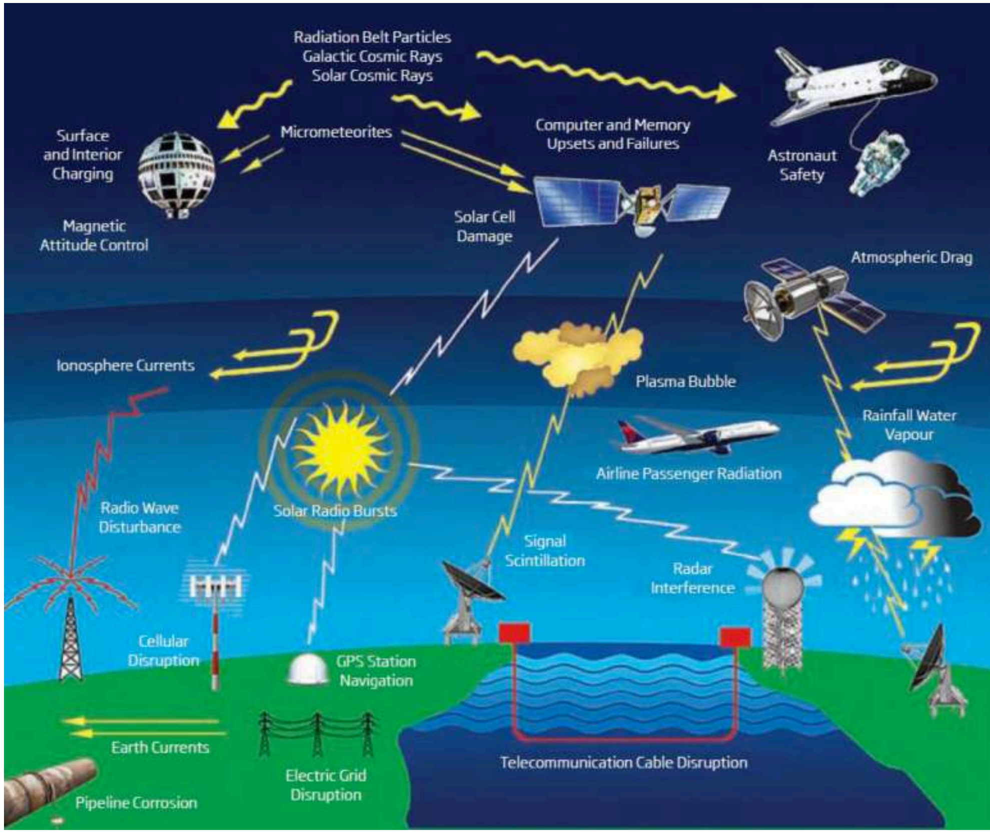

Impact on **nearby space** (satellites, astronauts)

Impact on **atmosphere** (communications, flights)

Impact on **ground** (electric grid, **networks**, pipelines/aquaduc/gasoduc)

→ If a Carrington (1859) event would arrive now, damages have been evaluated to be larger than 2 trillions $!!! (Loyds' report)

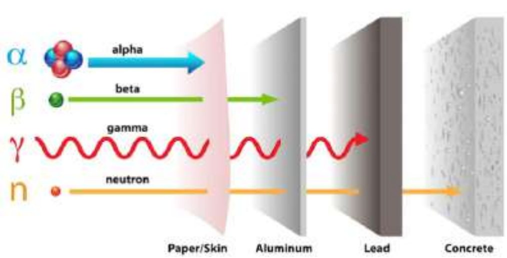

So need better models of the Sun

and how it controls the heliosphere

=>

Exascale supercomputers

=>

New Code Development

and International Benchmark Validation

2.5D model to capture the 11 yr cycle:

A&A 483, 949–960 (2008)
DOI: 10.1051/0004-6361:20078351
© ESO 2008

Astronomy & Astrophysics

A solar mean field dynamo benchmark

L. Jouve[1], A. S. Brun[1], R. Arlt[2], A. Brandenburg[3], M. Dikpati[4], A. Bonanno[5], P. J. Käpylä[3,7], D. Moss[6], M. Rempel[4], P. Gilman[4], M. J. Korpi[7], and A. G. Kosovichev[8]

Codes involves: STELEM, NDYND, MBRK, MESFISTO, HAO dynamo 1 & 2, CTDYN, HOLLERBACH

Table 1. Summary of the test cases, the cases followed by a prime have radial field boundary conditions (BC) at the top and the cases preceded by S are supercritical (computed with a value of C_α or C_s well above the dynamo threshold).

Case	Ω-effect	Poloidal source term	Diffusivity	Meridional flow	C_Ω	C_α	C_s	R_e	Top BC
A	Eq. (13)	α: Eq. (15)	$\tilde{\eta} = 1$ ($\eta_c = \eta_t$ in Eq. (14))	NO	1.40×10^5	$C_\alpha^{\rm crit}$(A)	0	0	Potential
A′	Eq. (13)	α: Eq. (15)	$\tilde{\eta} = 1$ ($\eta_c = \eta_t$ in Eq. (14))	NO	1.40×10^5	$C_\alpha^{\rm crit}$(A′)	0	0	Radial
SA′	Eq. (13)	α: Eq. (16)	$\tilde{\eta} = 1$ ($\eta_c = \eta_t$ in Eq. (14))	NO	1.40×10^5	3.5	0	0	Radial
B	Eq. (13)	α: Eq. (15)	Eq. (14)	NO	1.40×10^5	$C_\alpha^{\rm crit}$(B)	0	0	Potential
B′	Eq. (13)	α: Eq. (15)	Eq. (14)	NO	1.40×10^5	$C_\alpha^{\rm crit}$(B′)	0	0	Radial
SB′	Eq. (13)	α: Eq. (16)	Eq. (14)	NO	1.40×10^5	3.5	0	0	Radial
C	Eq. (13)	BL: Eq. (17)	Eq. (14)	Eq. (19)	1.40×10^5	0	$C_s^{\rm crit}$(C)	700	Potential
C′	Eq. (13)	BL: Eq. (17)	Eq. (14)	Eq. (19)	1.40×10^5	0	$C_s^{\rm crit}$(C′)	700	Radial
SC′	Eq. (13)	BL: Eq. (18)	Eq. (14)	Eq. (19)	1.40×10^5	0	35	700	Radial

Case	Code	Resolution	Δt	C_α^{crit}	ω
A	STELEM	65×65	10^{-5}	0.385	157
A	NDYND	81×81	5×10^{-6}	0.385	158
A	MBRK	81×81	5×10^{-6}	0.390	159
A	CTDYN	70×70 *	–	0.388	160
A	HAO2	101×101	10^{-5}	0.388	156
A	HOLLER	60×60 *	5×10^{-5}	0.385	159
Mean val				**0.387**	**158.1**
Std Dev.				**0.002**	**1.472**
R. S. D.				**0.006**	**0.009**
A′	STELEM	65×65	10^{-5}	0.366	158
A′	NDYND	81×81	5×10^{-6}	0.369	156
A′	MBRK	81×81	5×10^{-6}	0.372	158
A′	MEFISTO	121×121	10^{-6}	0.368	158
A′	HAO1	128×128	3×10^{-6}	0.368	157
Mean val				**0.369**	**157.4**
Std Dev.				**0.002**	**0.894**
R. S. D.				**0.006**	**0.006**

Test Accuracy of solutions and Boundary conditions

Agreement within 1%

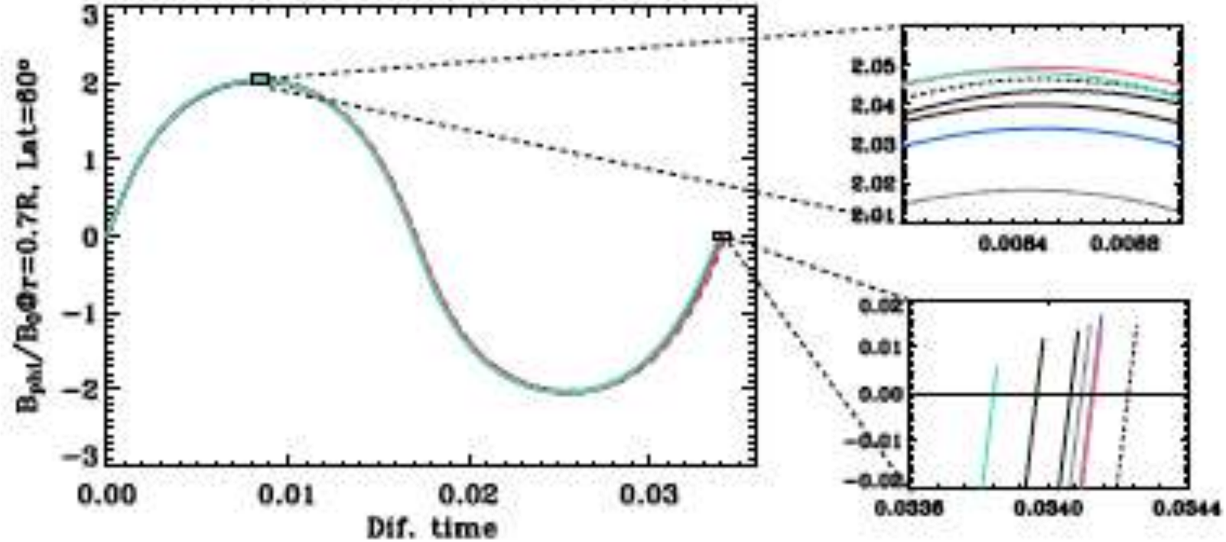

Test convergence with resolution

Table 4. Same as for Table 2, for cases C and C′.

Case	Code	Resolution	Δt	$C_\alpha^{\rm crit}$	ω
C	STELEM	129×129	10^{-6}	2.520	542
C	NDYND	81×81	10^{-6}	2.513	525
C	HAO2	101×101	10^{-5}	2.515	546
C	MBRK	151×151	10^{-6}	2.540	532
C	HOLLER	100×100 *	5×10^{-8}	2.355	538
Mean val				**2.489**	**536.6**
Std Dev.				**0.075**	**8.295**
R. S. D.				**0.03**	**0.015**
C′	STELEM	129×129	10^{-6}	2.460	544
C′	NDYND	321×321	5×10^{-7}	2.469	534
C′	MBRK	256×256	5×10^{-7}	2.473	537
C′	MEFISTO	201×201	10^{-6}	2.463	539
C′	HAO1	128×128	3×10^{-6}	2.450	537
Mean val				**2.463**	**538.2**
Std Dev.				**0.009**	**3.701**
R. S. D.				**0.004**	**0.007**

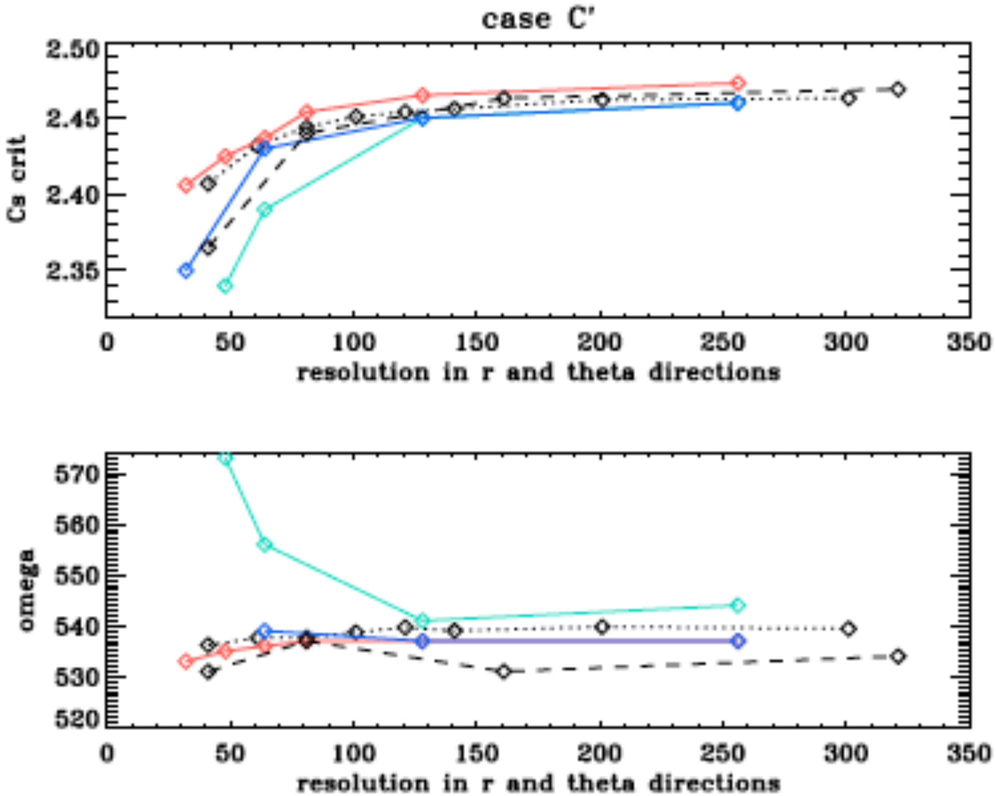

Agreement within 1%

More involved: 3D Convection and 3D Convective Dynamo

Icarus 216 (2011) 120–135

ELSEVIER

Contents lists available at SciVerse ScienceDirect

Icarus

journal homepage: www.elsevier.com/locate/icarus

Anelastic convection-driven dynamo benchmarks

C.A. Jones[a,*], P. Boronski[a], A.S. Brun[b], G.A. Glatzmaier[c], T. Gastine[d], M.S. Miesch[e], J. Wicht[d]

3. Polytropic reference state and the dimensionless formulation

With our assumption of gravity proportional to $1/r^2$, the anelastic equations admit an equilibrium polytropic solution,

$$\bar{\rho} = \rho_c \zeta^n, \quad \overline{T} = T_c \zeta, \quad \overline{P} = P_c \zeta^{n+1}, \quad \zeta = c_0 + \frac{c_1 d}{r}, \tag{18}$$

where n is the polytropic index, ζ_i and ζ_o are the values of ζ at the inner and outer boundaries respectively, $d = r_o - r_i$, and the constants c_0 and c_1 are defined by

$$c_0 = \frac{2\zeta_o - \beta - 1}{1 - \beta}, \quad c_1 = \frac{(1+\beta)(1-\zeta_o)}{(1-\beta)^2},$$
$$\zeta_o = \frac{\beta + 1}{\beta \exp(N_\rho / n) + 1}, \quad \zeta_i = \frac{1 + \beta - \zeta_o}{\beta}, \tag{19}$$

$$\frac{\partial \mathbf{u}}{\partial t} + \boldsymbol{\omega} \times \mathbf{u} = -\nabla\left(\frac{Pm}{E}\frac{p'}{\zeta^n} + \frac{1}{2}\mathbf{u}^2\right) + Pm\left[-\frac{2}{E}\hat{\mathbf{z}} \times \mathbf{u} + \frac{1}{E\zeta^n}(\nabla \times \mathbf{B}) \times \mathbf{B} + \mathbf{F}_v + \frac{PmRa}{Pr}\frac{S}{r^2}\hat{\mathbf{r}}\right] \tag{22}$$

where

$$\boldsymbol{\omega} = \nabla \times \mathbf{u}, \qquad \mathbf{F}_v = \zeta^{-n}\frac{\partial}{\partial x_j}\zeta^n\left(\frac{\partial u_i}{\partial x_j} + \frac{\partial u_j}{\partial x_i}\right) - \frac{2}{3}\zeta^{-n}\frac{\partial}{\partial x_i}\zeta^n\frac{\partial u_j}{\partial x_j}. \tag{23}$$

The dimensionless entropy equation becomes

$$\frac{DS}{Dt} = \frac{Pm}{Pr}\zeta^{-n-1}\nabla \cdot \zeta^{n+1}\nabla S + \frac{Di}{\zeta}\left[E^{-1}\zeta^{-n}(\nabla \times \mathbf{B})^2 + Q_v\right] \tag{24}$$

with the dissipation parameter Di defined as

$$Di = \frac{GM}{dT_c c_p}\frac{Pr}{PmRa} = \frac{c_1 Pr}{PmRa}, \quad Q_v = 2\left[e_{ij}e_{ij} - \frac{1}{3}(\nabla \cdot \mathbf{u})^2\right],$$
$$e_{ij} = \frac{1}{2}\left(\frac{\partial u_i}{\partial x_j} + \frac{\partial u_j}{\partial x_i}\right). \tag{25}$$

The dimensionless induction equation is then

$$\frac{\partial \mathbf{B}}{\partial t} = \nabla \times (\mathbf{u} \times \mathbf{B}) + \nabla^2 \mathbf{B}. \tag{26}$$

Coupled PDEs, 8 x 3D primary variables

Purely Hydrodynamical Case:

Agree on an exact set of parameters

$$Ra = \frac{GMd\Delta S}{\nu\kappa c_p}, \quad Pr = \frac{\nu}{\kappa}, \quad Pm = \frac{\nu}{\eta}, \quad E = \frac{\nu}{\Omega d^2},$$
$$N_\rho = \ln\left(\frac{\rho_i}{\rho_o}\right), \quad n, \quad \beta = \frac{r_i}{r_o},$$

Table 1
Parameters for the hydrodynamic benchmark. The chosen defining physical input values determine the conversion from dimensionless to dimensional units.

Dimensionless parameters
$E = 10^{-3}$, $N_\rho = 5$, $\beta = 0.35$, $Ra = 351{,}806$, $Pr = 1$, $n = 2$

Defining physical input values
$r_o = 7 \times 10^9$ cm, $\Omega = 1.76 \times 10^{-4}\,\mathrm{s}^{-1}$, $M = 1.9 \times 10^{30}$ g, $\rho_i = 1.1\,\mathrm{g\,cm}^{-3}$,
$\mathcal{R} = 3.503 \times 10^7\,\mathrm{erg\,g}^{-1}\,\mathrm{K}^{-1}$, $G = 6.67 \times 10^{-8}\,\mathrm{g}^{-1}\,\mathrm{cm}^3\,\mathrm{s}^{-2}$

Polytropic constants
$\zeta_o = 0.256465$, $\zeta_i = 3.124385$, $c_0 = -1.287800$, $c_1 = 2.375792$, $V = 14.598801$

Derived physical input values
$r_i = 2.45 \times 10^9$ cm, $d = 4.55 \times 10^9$ cm, $\nu = 3.64364 \times 10^{12}\,\mathrm{cm}^2\,\mathrm{s}^{-1}$,
$\kappa = 3.64364 \times 10^{12}\,\mathrm{cm}^2\,\mathrm{s}^{-1}$

Derived thermodynamic quantities in the model
$\rho_c = 0.112684\,\mathrm{g\,cm}^{-3}$, $\rho_o = 0.00741174\,\mathrm{g\,cm}^{-3}$, $T_i = 348{,}548$ K, $T_c = 111{,}557$ K,
$T_o = 28{,}611$ K,
$p_i = 1.343061 \times 10^{13}\,\mathrm{dyne\,cm}^{-2}$, $p_c = 4.403540 \times 10^{11}\,\mathrm{dyne\,cm}^{-2}$,
$p_o = 7.428259 \times 10^9\,\mathrm{dyne\,cm}^{-2}$,
$\Delta S = 851225.7\,\mathrm{erg\,g}^{-1}\,\mathrm{K}^{-1}$, $c_p = 1.0509 \times 10^8\,\mathrm{erg\,g}^{-1}\,\mathrm{K}^{-1}$, $\Delta S/c_p = 0.0081$,
Basic state luminosity $= 7.014464 \times 10^{32}\,\mathrm{erg\,s}^{-1}$

Dimensionless units
Velocity $800.8\,\mathrm{cm\,s}^{-1}$; time 5.681818×10^6 s; distance 4.55×10^9 cm;
energy 6.806845×10^{33} erg
Energy density $7.226228 \times 10^4\,\mathrm{erg\,cm}^{-3}$; luminosity $1.773999 \times 10^{32}\,\mathrm{erg\,s}^{-1}$

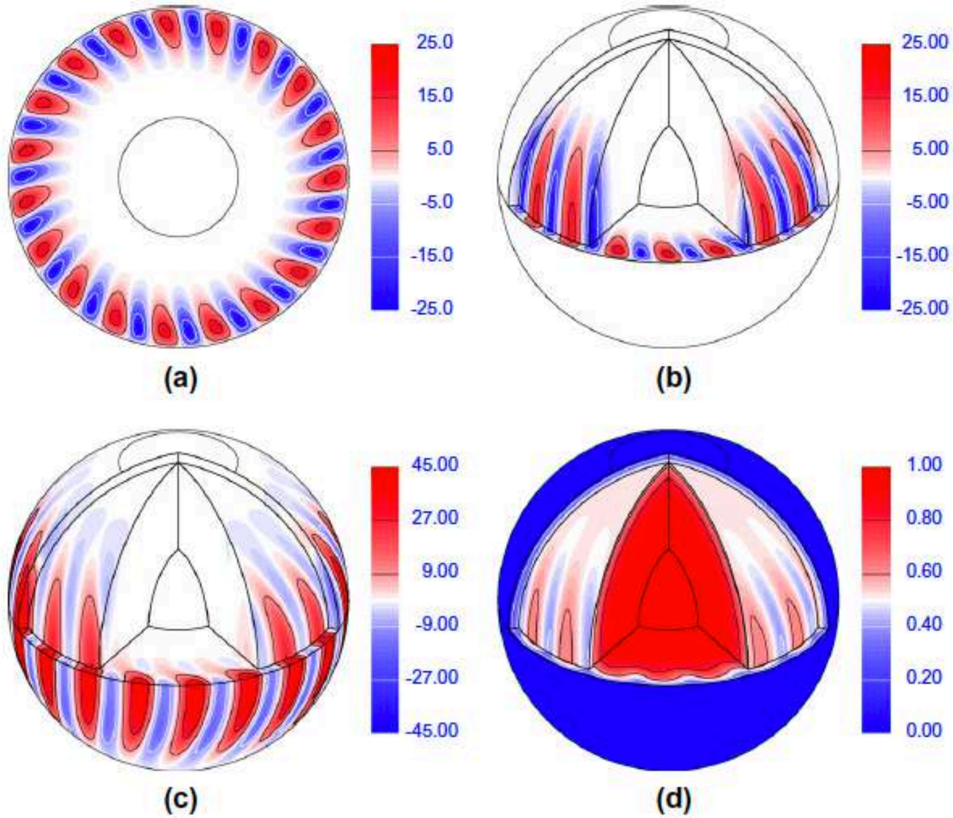

Wave-like behavior.

Jones et al. 2011

Testing integral values (global energies),
but also specific pointwise values

Table 2
Results from the hydrodynamic benchmark.

Code	Leeds	Glatzmaier	ASH	MAGIC
K.E. (erg)	5.57195×10^{35}	5.57028×10^{35}	5.52650×10^{35}	5.57062×10^{35}
K.E. dimensionless	81.8581	81.8335	81.1903	81.8385
K.E. density (erg cm^{-3})	4.05188×10^{5}	4.05066×10^{5}	4.01882×10^{5}	4.05091×10^{5}
Luminosity (erg s^{-1})	7.44878×10^{32}	7.44878×10^{32}	7.44877×10^{32}	7.44880×10^{32}
Luminosity dimensionless	4.19886	4.19886	4.19886	4.19887
Zonal K.E. (erg)	6.38294×10^{34}	6.38099×10^{34}	6.33063×10^{34}	6.38151×10^{34}
Zonal K.E. dimensionless	9.37724	9.37437	9.30039	9.37514
Meridional K.E. (erg)	1.49875×10^{32}	1.49825×10^{32}	1.48637×10^{32}	1.49843×10^{32}
Meridional K.E. dimensionless	0.0220183	0.0220109	0.0218364	0.0220136
Period τ dimensional (days)	1.23264	1.23263	1.23263	1.23241
Period τ dimensionless	0.0187440	0.0187440	0.0187439	0.0187404
$\omega = 2\pi/19\tau$ (rad s^{-1})	3.10511×10^{-6}	3.10512×10^{-6}	3.10512×10^{-6}	3.10570×10^{-6}
$\omega = 2\pi/19\tau$ dimensionless	17.6427	17.6427	17.6428	17.6460
u_ϕ at $u_r = 0$ (cm s^{-1})	690.15	690.27	687.65	689.66
u_ϕ at $u_r = 0$ dimensionless	0.86183	0.86197	0.85871	0.86122
S at $u_r = 0$ (erg g^{-1} K^{-1})	7.9420×10^{5}	7.9452×10^{5}	7.9766×10^{5}	7.9452×10^{5}
S at $u_r = 0$ dimensionless	0.93301	0.93338	0.93707	0.93338
Resolution	$128 \times 192 \times 384$	$121 \times 512 \times 1024$	$129 \times 256 \times 512$	$121 \times 192 \times 384$
Timestep (s)	14.2	33	33	28.41
Timestep dimensionless	2.5×10^{-6}	5.8×10^{-6}	5.8×10^{-6}	5×10^{-6}
Run length (days)	92	450	154.4	197.29
Run length dimensionless	1.4	6.8	2.35	3.0

Agreement within 1%, sometimes better

MHD mode validation + turbulence state

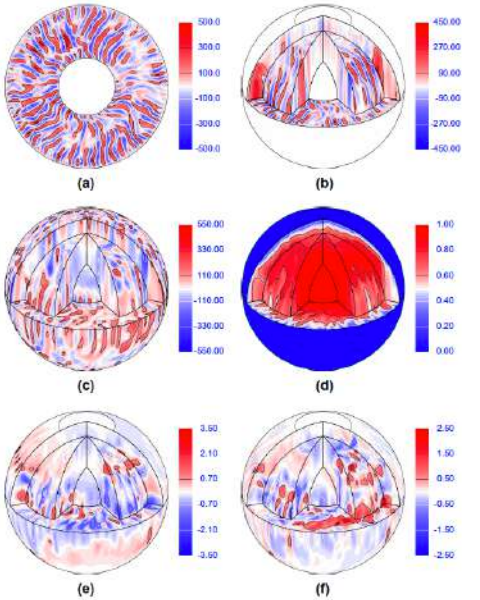

- Highly stratified system requires long integration time
- Turbulent state implies long temporal averages to compare outputs

Agreement within 1%, sometimes better

Table 6
Results from the unsteady dynamo benchmark. Time-averaged values are shown, with the corresponding standard deviation in square brackets, expressed as a percentage of the average value.

Code	Leeds	Glatzmaier	ASH	MAGIC
M.E. (erg)	1.81×10^{36} [12%]	1.80×10^{36} [10%]	1.77×10^{36} [13%]	1.84×10^{36} [11%]
M.E. dimensionless	2.42×10^{5} [12%]	2.40×10^{5} [10%]	2.37×10^{5} [13%]	2.46×10^{5} [11%]
K.E. (erg)	1.74×10^{36} [13%]	1.75×10^{36} [12%]	1.72×10^{36} [12%]	1.74×10^{36} [12%]
K.E. dimensionless	2.32×10^{5} [13%]	2.34×10^{5} [12%]	2.29×10^{5} [12%]	2.32×10^{5} [12%]
Zonal M.E. (erg)	7.07×10^{34} [40%]	7.07×10^{34} [38%]	7.12×10^{34} [34%]	7.10×10^{34} [41%]
Zonal M.E. dimensionless	9.45×10^{3} [40%]	9.45×10^{3} [38%]	9.51×10^{3} [34%]	9.49×10^{3} [41%]
Meridional M.E. (erg)	1.59×10^{35} [43%]	1.66×10^{35} [33%]	1.53×10^{35} [38%]	1.67×10^{35} [44%]
Meridional M.E. dimensionless	2.13×10^{4} [43%]	2.22×10^{4} [33%]	2.04×10^{4} [38%]	2.23×10^{4} [44%]
Zonal K.E. (erg)	1.02×10^{35} [37%]	1.00×10^{35} [43%]	1.02×10^{35} [55%]	1.02×10^{35} [38%]
Zonal K.E. dimensionless	1.36×10^{4} [37%]	1.34×10^{4} [43%]	1.36×10^{4} [55%]	1.36×10^{4} [38%]
Meridional K.E. (erg)	7.84×10^{32} [31%]	8.36×10^{32} [30%]	8.90×10^{32} [29%]	8.28×10^{32} [32%]
Meridional K.E. dimensionless	105 [31%]	112 [30%]	119 [29%]	111 [32%]
Luminosity ($erg\,s^{-1}$)	4.62×10^{31}	4.67×10^{31}	4.65×10^{31}	4.64×10^{31}
Luminosity dimensionless	42.5	43.0	42.8	42.7
Standard deviation (bottom)	11%	11%	9%	11%
Standard deviation (top)	4%	4%	3%	5%
Resolution	$96 \times 288 \times 576$	$129 \times 256 \times 512$	$129 \times 256 \times 512$	$121 \times 256 \times 512$
Timestep (s)	681	100	100	113.64
Timestep dimensionless	3×10^{-6}	4.4×10^{-7}	4.4×10^{-7}	5×10^{-7}
Run length (days)	3950	1022	2014	3644
Run length dimensionless	1.5	0.39	0.77	1.35

New Code: Dyablo for exascale machines

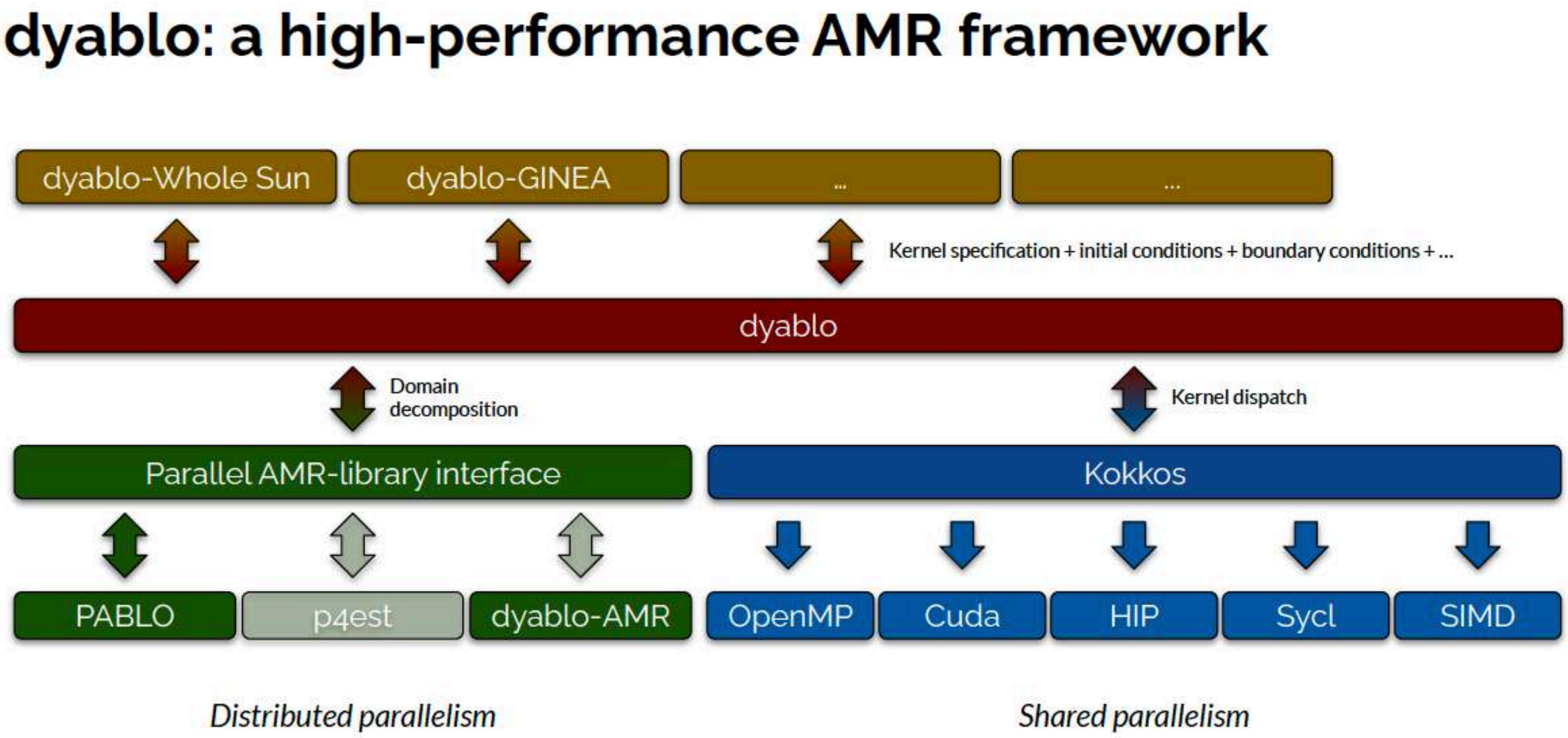

CEA/DRF/IRFU HPC activities
Computational Astrophysics (COAST) program

Dyablo-Whole Sun: Performance study

Sedov-Blasts in 3D. Max-resolution per blast 512^3
Run on Jean-Zay Intel Cascade Lake 6248 CPUs (40 cores per node); 4 MPI processes per node

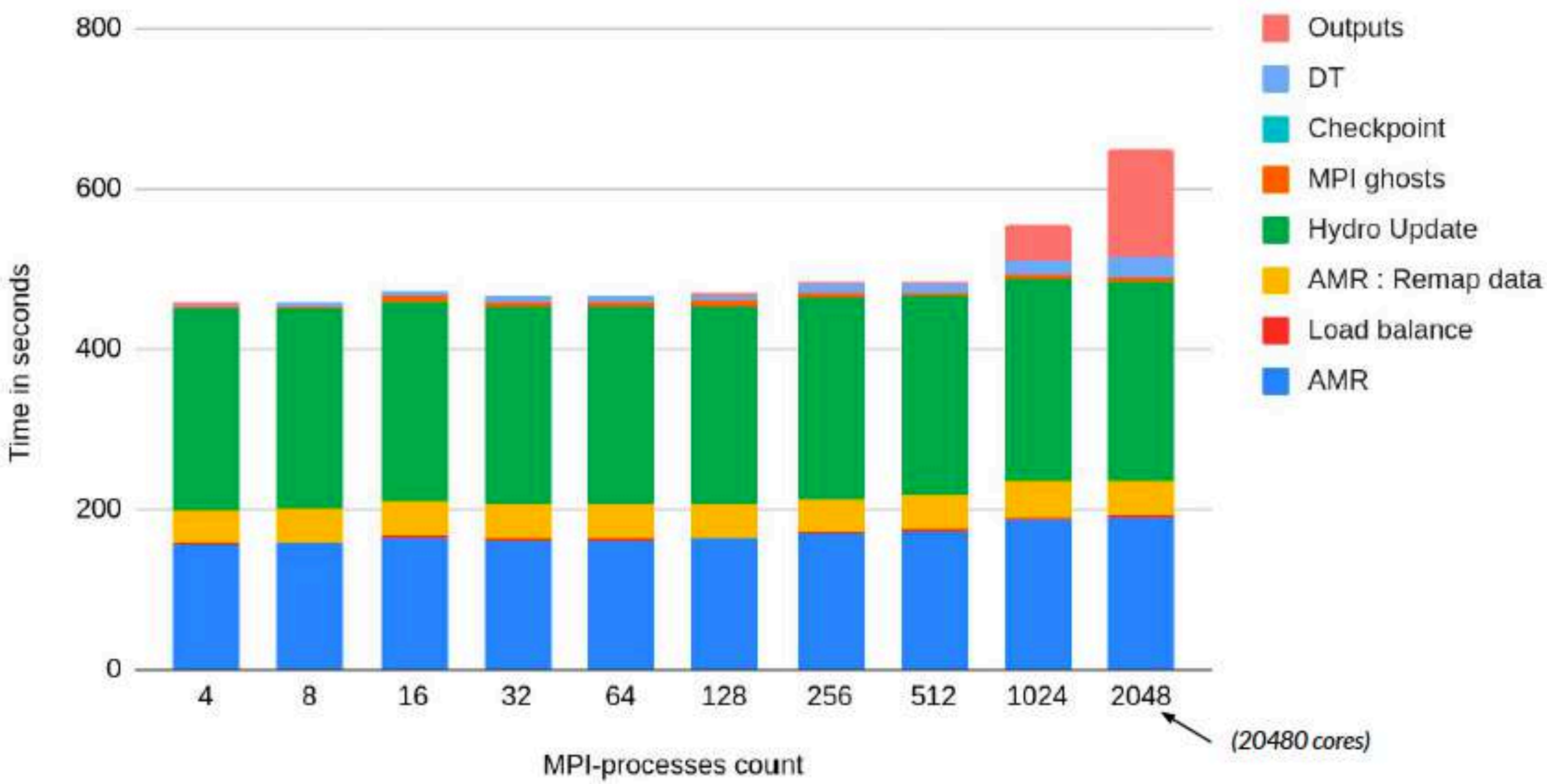

20480 gpu cores

A. Durocher, M. Delorme (CEA/IRFU)

Convection at various Reynolds number (fixed grid)

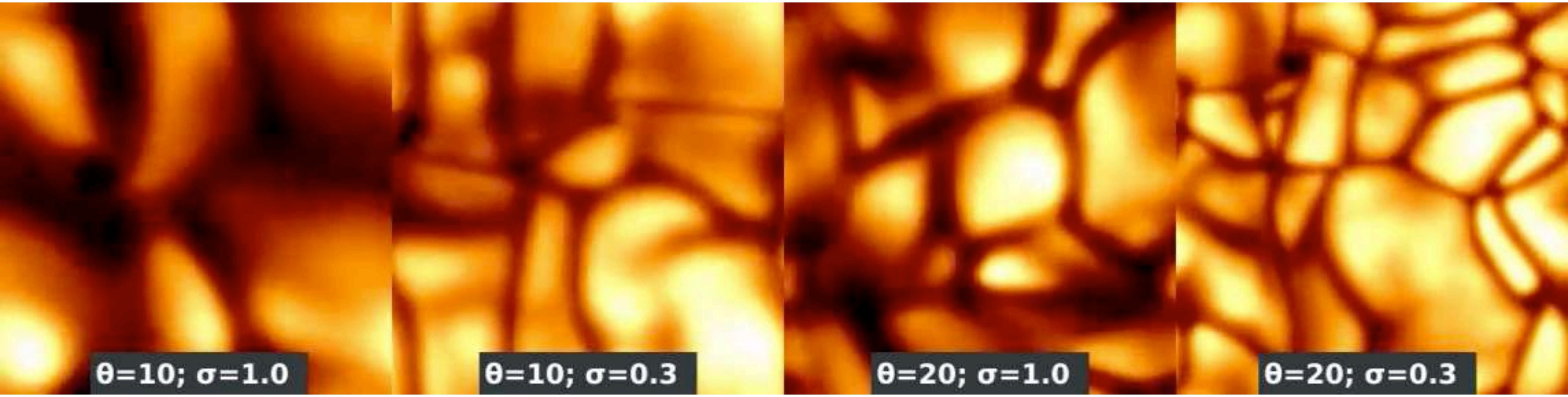

Setup inspired by Cattaneo et al. 1991, Astrophysical Journal, 370, 282

Using relatively old published papers sometimes leads to Pb:
Such as not well defined quantities or setups or unclear time or location of probing or plotting of figures

ercWHOLE

9 Codes involved

Convection Benchmark

Code	Solver type	Benchmarking institute
Dedalus	Spectral methods	UCB
Dispatch/HLLS	Finite-volumes/Finite-differences	ROCS
dyablo-Whole Sun	Finite-volumes	CEA
HPS	Spectral methods	USCS
Idefix	Finite-Volume	IPAG
Lare3d	Finite-differences	University of St. Andrews
MURaM/Yuto's	Finite-differences	MPS
PLUTO	Finite-volumes/Finite-differences	CEA
R2D2	Finite-differences	Chiba University

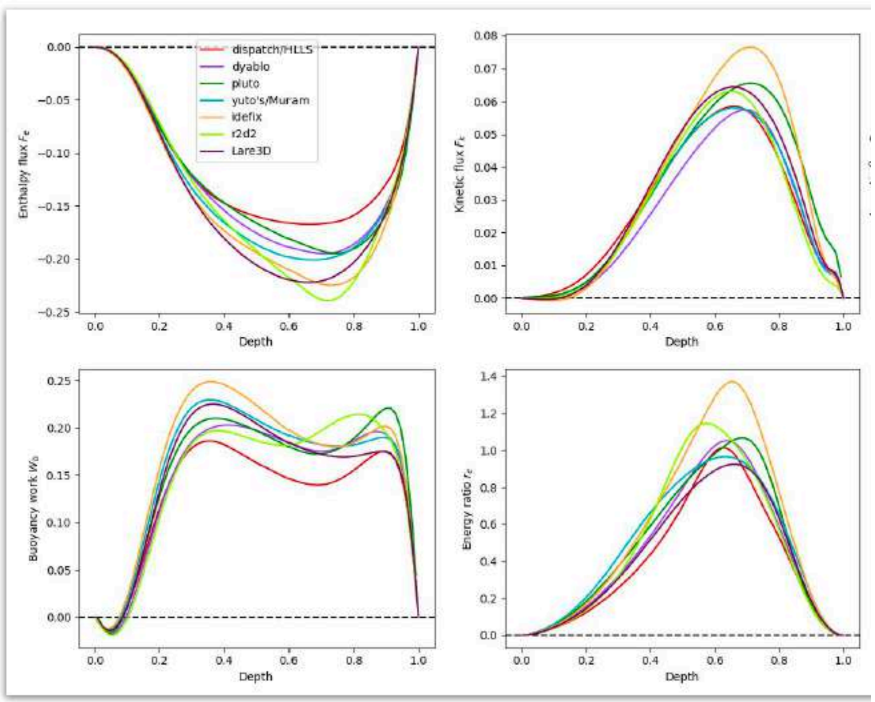

First convection with AMR run on GPUs

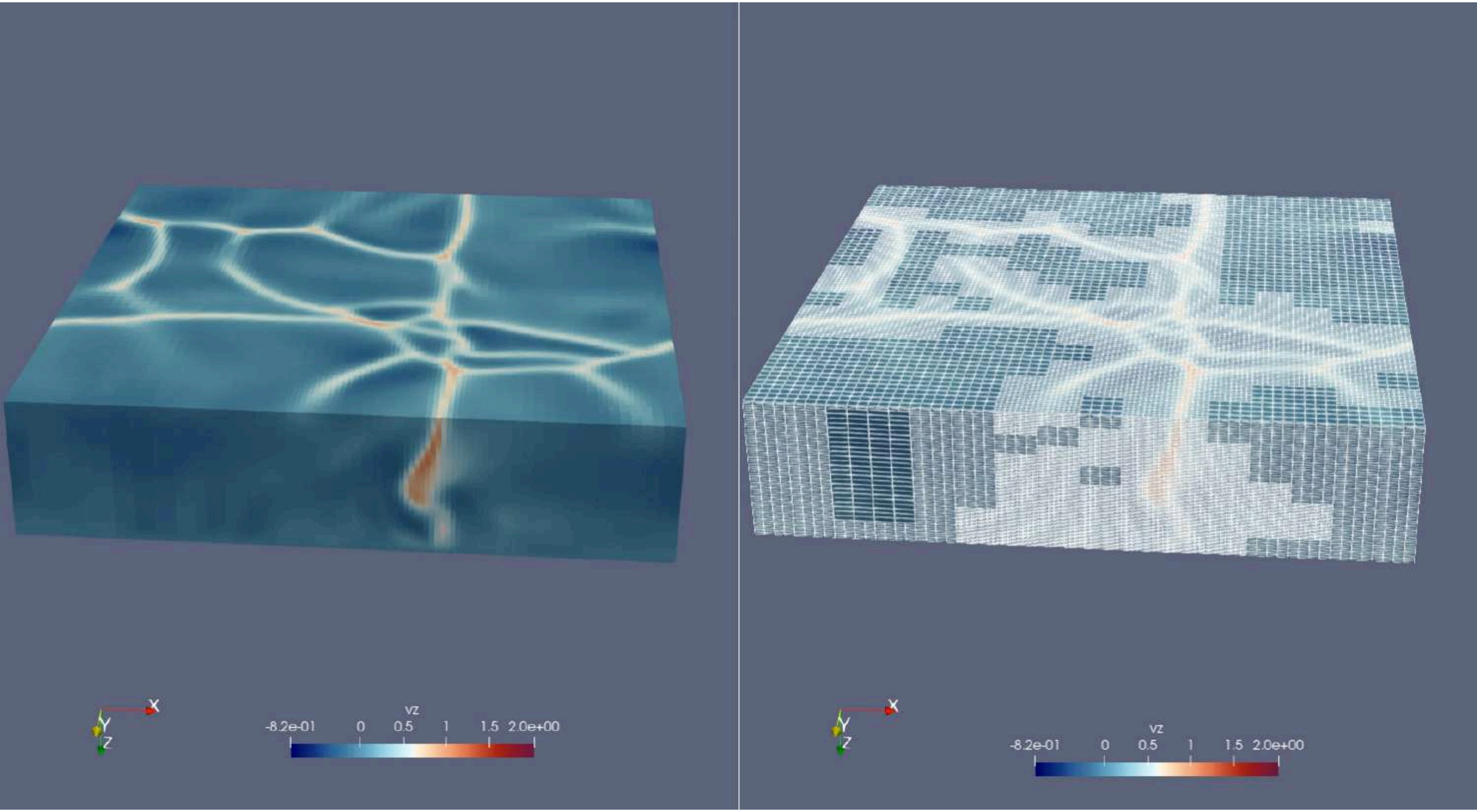

Brun, Delorme, Finley

Another version with Newton Cooling

Testing hydrostatic equilibrium
in fully compressible Finite Volume code (well-balanced scheme)

4 codes: 2 fixed grids, 2 AMR

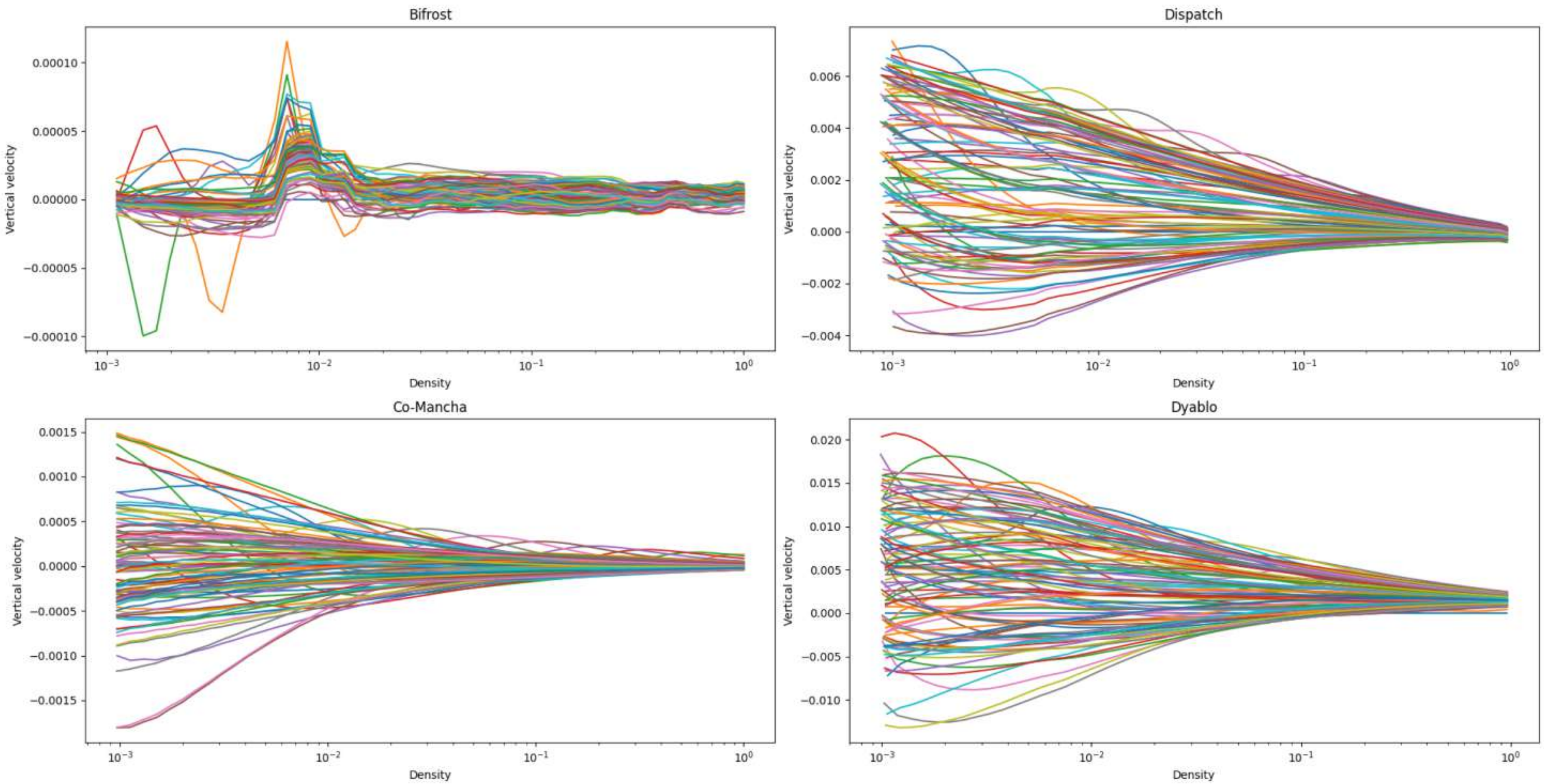

Comparison with Community Standard Code (no AMR) and new solar AMR codes

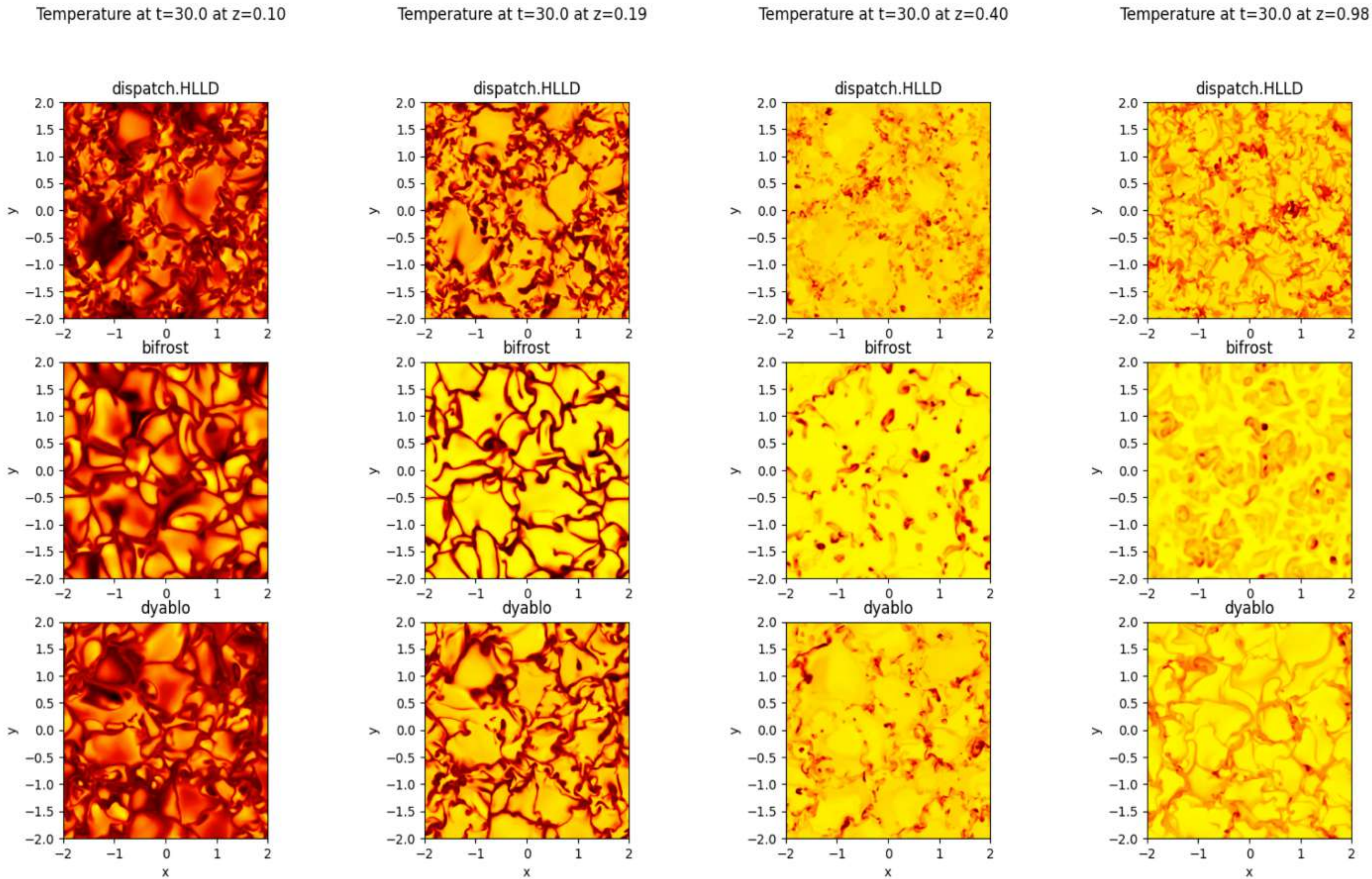

Unitary Tests: Checking Various MHD Solvers

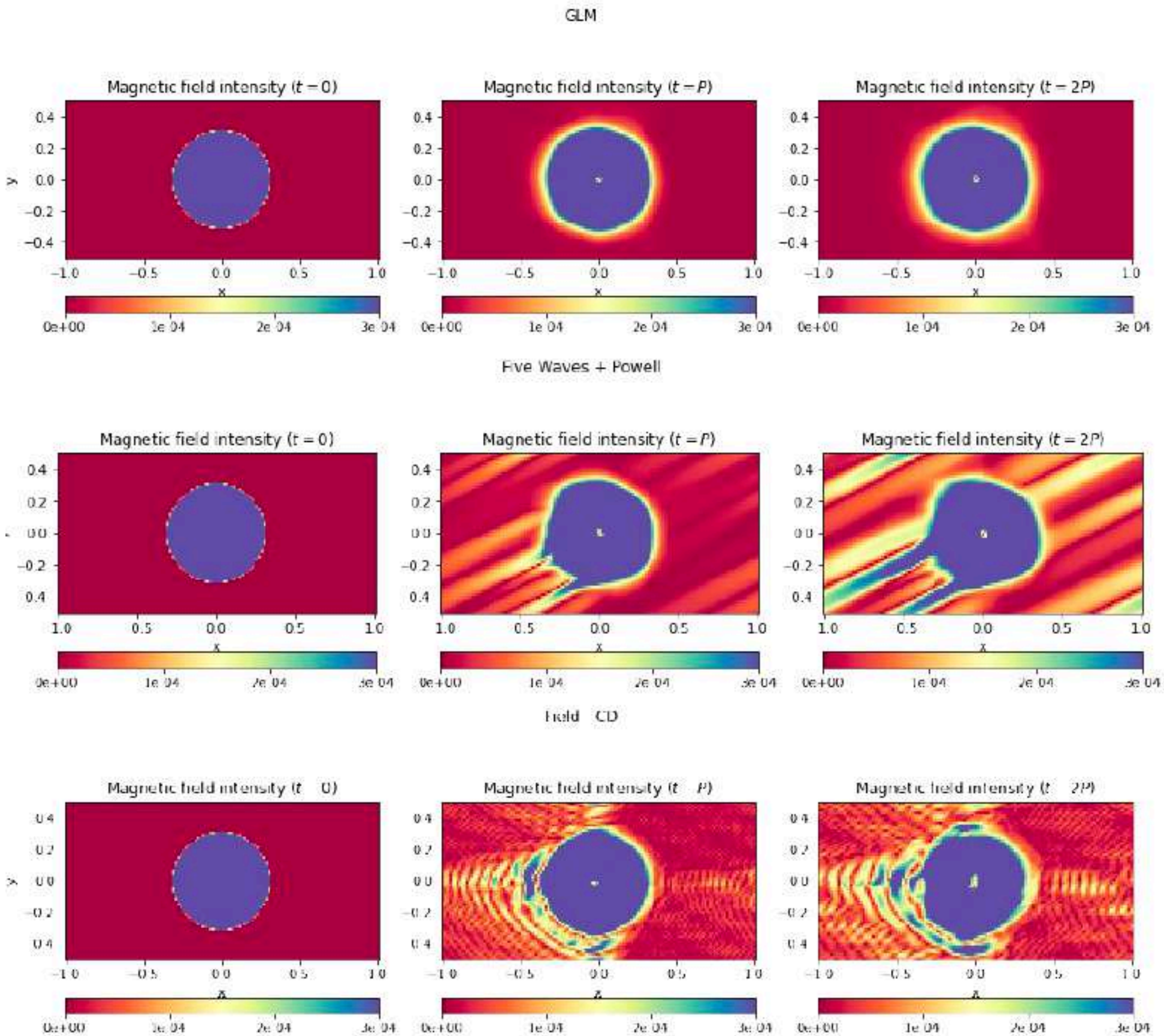

All Mach MHD Regime Most needed => Work in progress

First small scale dynamo with AMR

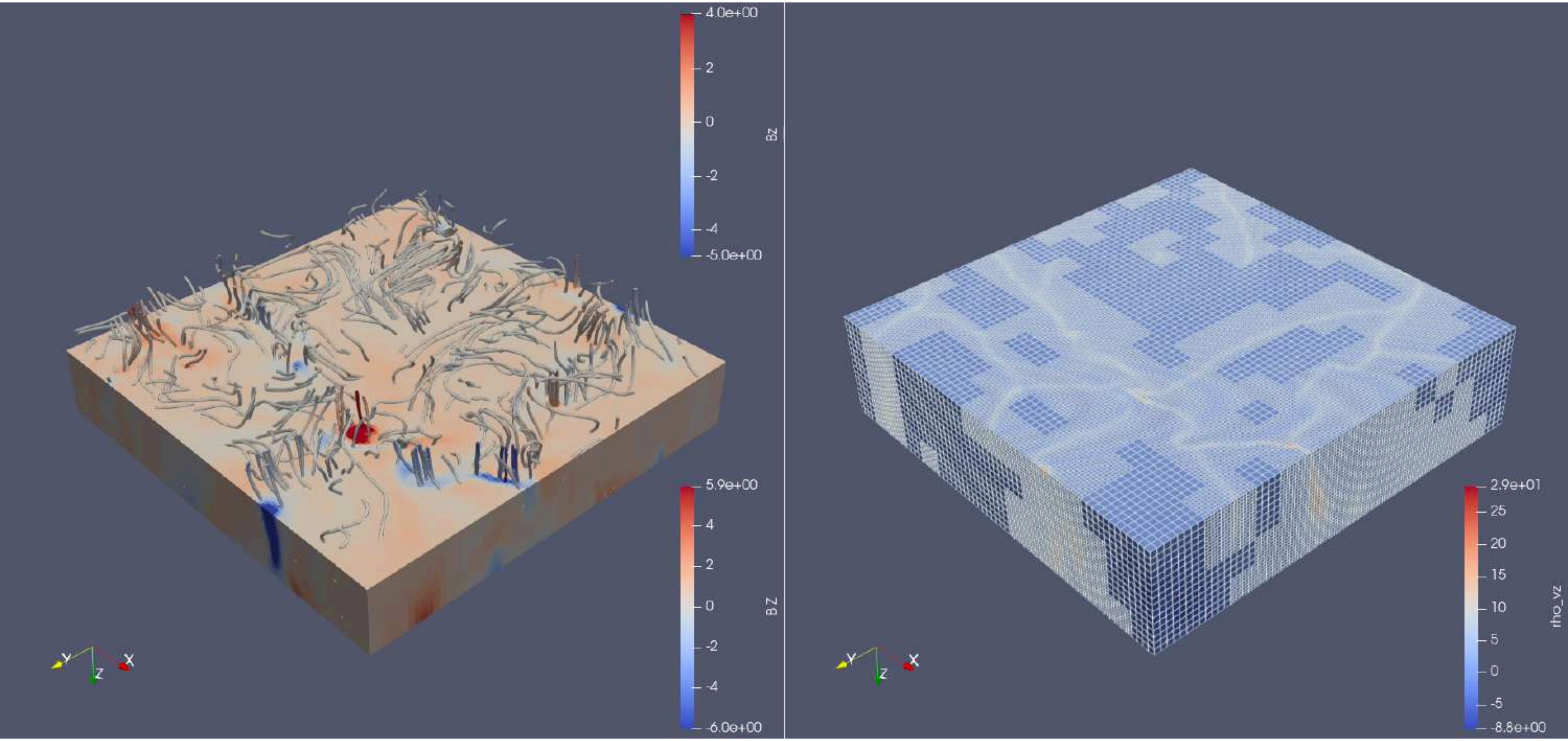

Dynamo benchmark will follow up the convection benchmark

Going spherical:
isomorphism between unitary AMR cube and shell/ring/sphere

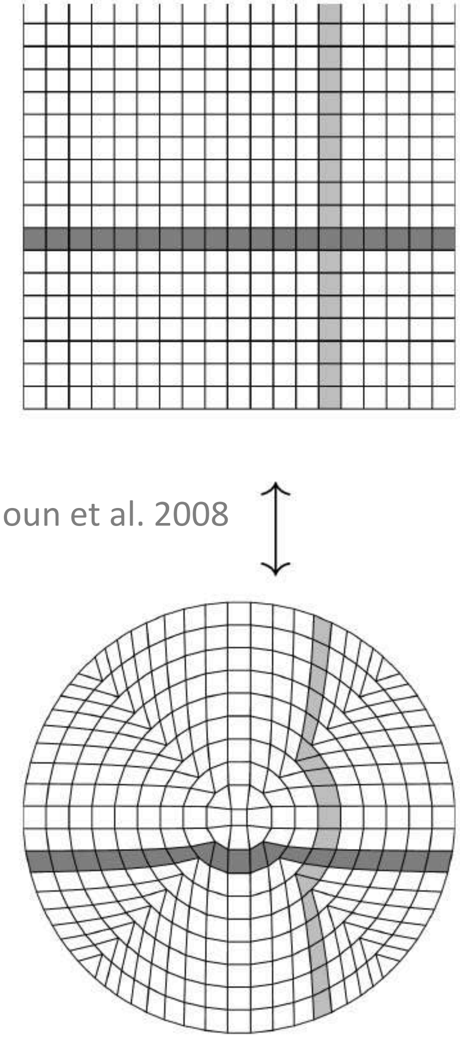

Calhoun et al. 2008

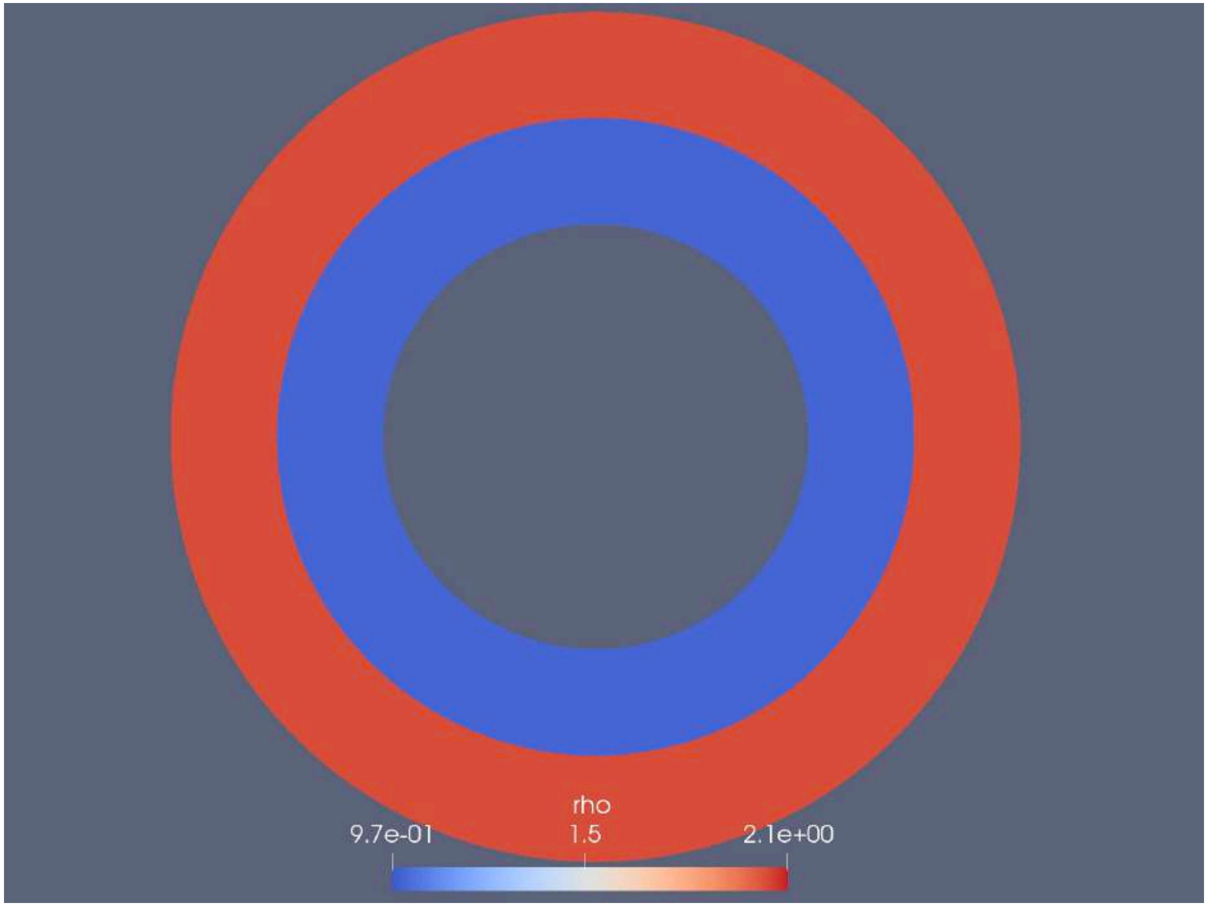

Doebele, Delorme, Brun 2023

Conclusions

Understanding the Sun and its heliosphere is key for our modern society

Solar activity can have major impacts on Earth, even on supercomputers!
(solar energetic particles or GICs can dammage network and processors)

Developing exa-scale (and beyond) ready solar plasma codes is critical to describe our star (high degrees of turbulence, large range of temporal/spatial scales, multi physics and multi regimes, radiative transfer, high energy particles ….)

Unitary Tests and International Benchmarks are most needed to achieve such ambitious goal as there are too many ways of doing something wrong…..

Extra Slide

Kokkos: performance portability in C++

A solution to heterogeneous systems

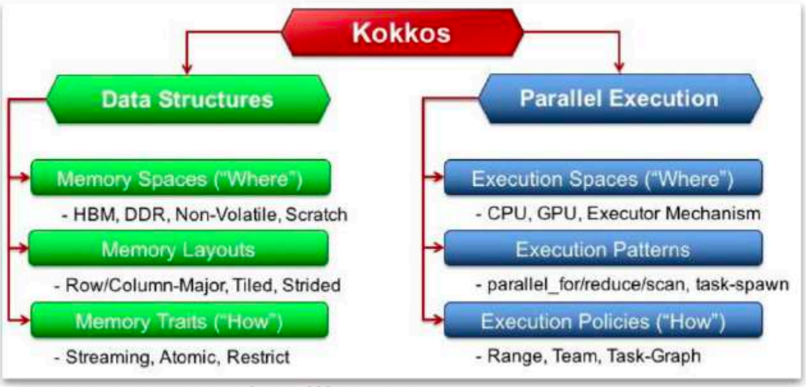

- Open-source modern C++ metaprogramming library
- Developer picks the memory structure, the type of algorithm and provides computation kernels
- Kokkos provides backends to automatically adapt the code to target architectures with minimum overhead

https://github.com/kokkos/kokkos
Carter Edwards, H., Trott, C., Sunderland, D., "Kokkos: Enabling manycore performance portability through polymorphic access patterns", Journal of Parallel and Distributed Computing, 2014